ACES Asian Chemical Editorial Society

doi.org/10.1002/ajoc.202300347

ASIAN JOURNAL OF ORGANIC CHEMISTRY
Research Article

www.asianjoc.org

Special Collection

Dual Photosensitizer Cycles Working Synergistically in a C(sp)-C(sp^3) Cross-Coupling Reaction**

Megan Amy Bryden,[a] Marco Villa,[b, c] Andrea Fermi,[b, c] Paola Ceroni,*[b, c] and Eli Zysman-Colman*[a]

To assess the value and reactivity of new photocatalysts (PCs), their performance should be evaluated in one or more established reactions and benchmarked against the performance using known PCs. Here, we evaluated our recently developed PC, **pDTCz-DPmS**, in a C(sp)-C(sp^3) cross-coupling reaction that had been documented in the literature. Previous findings indicated this reaction could not proceed in the absence of PC; however, under our conditions this was not the case. Without PC, a moderate product yield was obtained, while this yield increased significantly upon addition of **pDTCz-DPmS**. UV-Vis absorption studies indicated that the Hantzsch ester (HE) additive was acting as a competitive absorber of the light from the excitation source, and quenching studies confirmed that the HE was quenched by the radical precursor, *N*-(acyloxy)phthalimide. Mechanistic investigations established that two parallel photosensitization pathways were in operation; a reductive quenching photocatalytic pathway (using **pDTCz-DPmS**) and a sacrificial photoreductant pathway (employing HE). These pathways work synergistically to enhance the yield of target product.

Introduction

Progress in photocatalysis over the last two decades has been extensive, allowing it to emerge as a commonly employed tool in organic synthesis.[1–6] A plethora of reactions have been developed that proceed photocatalytically, from the photocatalytic splitting of water[7] to the C(sp^3)-functionalization of substrates.[8] Despite the wide array of transformations that can be conducted using photocatalysis, due to the heterogeneity of photoreactor setups coupled with the paucity of direct experimental evidence to support the putative photocatalytic mechanism advanced in many reports, it can become difficult to replicate the reported outcomes of photoreactions.

The challenges facing further development of photocatalysis, including reaction setup, reaction scale-up, optoelectronic characterisation of the photocatalyst (PC), mechanistic investigation and caveats concerning reaction yields, have been recently discussed.[9,10] In the context of replicating a literature photocatalytic reaction and understanding the resultant yields obtained, the reaction setup and mechanistic evidence for said reaction become points of critical importance. Differences in yield when repeating literature photoreactions are to be expected since factors such as temperature, light source, and stirring rate can influence the reaction outcome.[11–13] Moreover, limited evidence is often provided to corroborate the putative mechanism, leaving doubt as to whether the reaction proceeds via the proposed photocatalytic cycle or whether other pathways may be plausible, as already discussed in recent reports.[14–18]

The importance of these factors came into stark relief during our assessment of the reactivity of the PC, 9,9′-(sulfonylbis(pyrimidine-5,2-diyl))bis(3,6-di-*tert*-butyl-9*H*-carbazole), **pDTCz-DPmS** (Figure 1).[19] We previously demon-

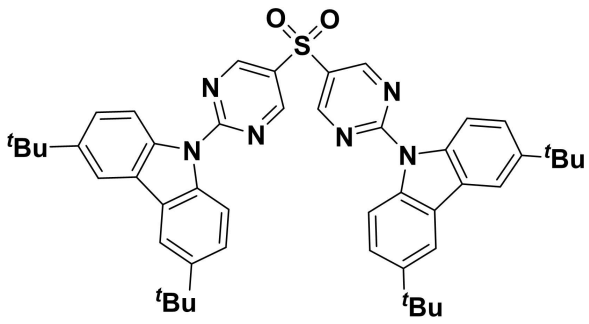

pDTCz-DPmS

Figure 1. Structure of **pDTCz-DPmS**, first reported in Ref. [20].

[a] *M. A. Bryden, Prof. Dr. E. Zysman-Colman*
Organic Semiconductor Centre, EaStCHEM School of Chemistry
University of St Andrews
St Andrews, Fife, KY16 9ST (UK)
E-mail: eli.zysman-colman@st-andrews.ac.uk
Homepage: http://www.zysman-colman.com

[b] *Dr. M. Villa, Dr. A. Fermi, Prof. Dr. P. Ceroni*
Department of Chemistry Ciamician
University of Bologna
Via Selmi 2, 40126 Bologna (Italy)

[c] *Dr. M. Villa, Dr. A. Fermi, Prof. Dr. P. Ceroni*
Center for Chemical Catalysis–C3
University of Bologna
via Selmi 2, 40126 Bologna (Italy)

[**] *A previous version of this manuscript has been deposited on a preprint server (https://doi.org/10.26434/chemrxiv-2023-bjmh1).*

Supporting information for this article is available on the WWW under https://doi.org/10.1002/ajoc.202300347

This manuscript is part of a special collection on Photo(redox) Catalysis.

strated that **pDTCz-DPmS** was a capable PC across a range of reactions covering disparate photocatalytic mechanisms: oxidative quenching, reductive quenching, energy transfer photocatalysis and dual metallaphotoredox catalysis with a Ni(II) co-catalyst, generally replicating or outcompeting the literature PC in terms of yield under similar reaction conditions.

One of the reactions that was probed was the C(sp)-C(sp^3) cross-coupling of bromoalkynes with *N*-(acyloxy)phthalimides (Figure 2). First reported by Yang *et al.* using $[Ru(bpy)_3](PF_6)_2$ as the PC (Figure 2a), the authors found that the activation of bromoalkynes was challenging, instead focusing on sulfonyl alkynes (28 vs 76% for coupling of *N*-(acyloxy)phthalimides with bromoalkynes and sulfonyl alkynes, respectively).[21] The reaction was conducted over 30 minutes in dichloromethane under 4 W 468 nm (blue) LED irradiation, placed 10 cm from the reaction vial.

The putative mechanism (see Scheme 1) implicated that either di*iso*propylethylamine (DIPEA) or the Hantzsch ester (HE) would reductively quench the PC given that such sacrificial reductants are so easy to oxidize[($E(DIPEA^{\bullet+}/DIPEA) = 0.81$ V vs SCE[22] and $E(HE^{\bullet+}/HE) = 1.00$ V vs SCE[23]]. This was supported by Stern-Volmer quenching, which identified both could quench the excited PC. The absence of either DIPEA or HE resulted in a decrease in the yield for sulfonyl alkynes, from 76 to 37% (for no DIPEA) and 28% (for no HE), with no product forming when both DIPEA and HE were removed. As such, it was concluded that both sacrificial reductants were necessary for the reaction. Closure of the photocatalytic cycle was proposed to occur through single electron transfer (SET) from the reduced PC to the *N*-(acyloxy)phthalimide, which typically have reduction potentials ranging from $E_{red} = -1.26$ V to -1.37 V vs SCE.[24]

Minozzi *et al.* subsequently studied the suitability of a large family of heteroleptic Cu(I) PCs[25] in this reaction and found that only four out of the 40 copper complexes tested could yield greater than 50% of the desired alkyne when using bromoalkynes as the coupling partner (Figure 2b), and only one

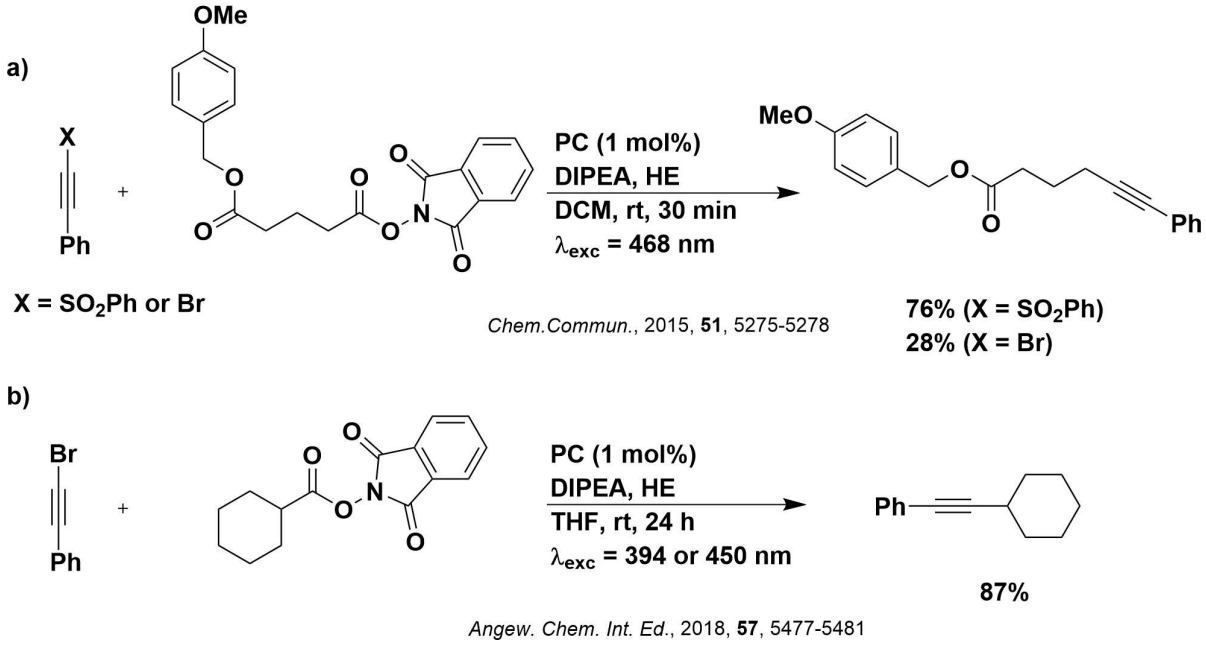

Figure 2. Literature reaction schemes for the C(sp)-C(sp^3) cross-coupling reaction between bromo- or sulfonyl-alkynes and *N*-(acyloxy)phthalimides.

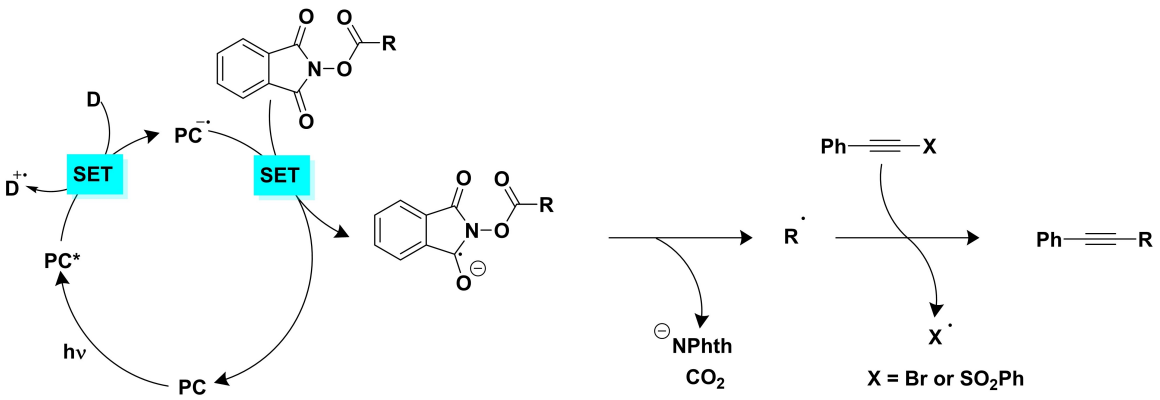

Scheme 1. Putative reaction mechanism for the C(sp)-C(sp^3) cross-coupling reaction, first proposed in Ref. [24].

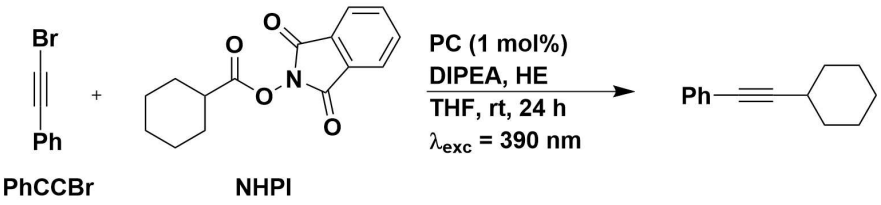

Figure 3. Reaction scheme for the photocatalytic C(sp)-C(sp^3) cross-coupling reaction of (bromoethynyl)benzene (PhCCBr) with the *N*-(acyloxy)phthalimides (NHPI) 1.3-dioxoisoindolin-2-yl cyclohexanecarboxylate.

of these complexes, [Cu(dq)(BINAP)]BF_4 [dq = 2,2′-biquinoline and BINAP = (±)-2,2′- bis(diphenylphosphino)-1,1′-binaphthalene], could provide a yield greater than 70%. The reaction was conducted in THF over 24 hours using 394 or 450 nm LED flexible strips of 72 W per 5 m spool. No mechanistic studies were conducted, and the authors could find no correlation of the yield with the photophysical/electrochemical properties of the Cu(I) complexes.

From a thermodynamic analysis, we expected **pDTCz-DPmS** to perform well in this reaction, particularly in the reduction of the *N*-(acyloxy)phthalimide (since $E_{red} = -1.65$ V vs SCE in THF for **pDTCz-DPmS**).[19] Herein, we report how divergent mechanisms for the same reaction are accessible and how this complicates the comparison of performance of different PCs.

Table 1. ^{1}H NMR yields obtained in the C(sp)-C(sp^3) cross-coupling reaction with various photocatalysts and relevant redox potentials.[a]

Photocatalyst	E_{red} [V]	E^*_{red} [V]	^{1}H NMR yield [%]
pDTCz-DPmS	−1.77[b]	1.32[b]	73±1
[Cu(dmp)(xantphos)]PF_6	−1.72[d]		62±3 (11)[c]
None	N/A	N/A	47±3 (no reaction)[c]

[a] Redox potentials are reported vs SCE and were obtained in THF unless otherwise noted. Reactions conditions followed as shown in Figure 3, for more details consult the SI. Values in parentheses indicate the isolated yield obtained in the literature and are referenced accordingly. [b] Value taken from Ref. [19]. [c] Value taken from Ref. [25] using flexible purple LED strips in THF. [d] Value taken from Ref. [27] in MeCN.

Results and Discussion

Photocatalysis investigations

Since Yang *et al.*[21] employed [Ru(bpy)$_3$]$(PF_6)_2$ as the PC, an excitation at 468 nm was used throughout their study. By contrast, the higher energy absorption onset of the Cu(I) complexes studied by Minozzi *et al.*[25] meant that excitation at 394 nm was more suitable for most of their PCs. Since the absorption profile of **pDTCz-DPmS** is more similar to those of the Cu(I) complexes, the conditions of Minozzi *et al.* were replicated in the present study. As such, Kessil lamps of 390 nm wavelength were chosen for photoexcitation in our photoreactor and the substrates investigated were (bromoethynyl)benzene and 1,3-dioxoisoindolin-2-yl cyclohexanecarboxylate (Figure 3), which have been abbreviated to PhCCBr and NHPI, respectively, in the subsequent discussion.

A significantly different yield was obtained in our set-up compared to that of Minozzi *et al.* when using [Cu(dmp)(xantphos)]PF_6 [dmp = 2,9-dimethyl-1,10-phenanthroline and xantphos = 4,5bis(diphenylphosphino)-9,9-dimethylxanthene] as the PC (62% vs. 11% reported by Minozzi *et al.*, Table 1), likely a result in part of the different reaction setups. Primarily, the photon flux of the light sources used (390 nm Kessil PR160 L vs purple LED flexible strips, for the two setups, respectively)[25] vary considerably and are probably the main culprit for the discrepancy in yield. Generally, higher intensity light sources give greater product yields, as shown in the study of König and co-workers using a series of commercial photoreactors.[11] From the description of the literature reaction setup, it is not possible to ascertain accurately what is the incident photon flux on the reaction vessel, a key parameter in photocatalysis.[26] As such, it becomes difficult to compare the yields obtained in our set-up with those obtained by others, signifying the importance of replicating literature reactions in ones own set-up to enable a meaningful cross-comparison of the yields with different PCs.

Replacement of [Cu(dmp)(xantphos)]PF_6 with **pDTCz-DPmS** as the PC allowed for a higher yield of 73% to be obtained in our setup, a result ostensibly of its suitable redox potentials (Table 1). However, there is a significant background reaction where in the absence of PC, a moderate yield of 47% was achieved using our photoreactor, while no formation of product was reported using the literature conditions for this control reaction.

We next conducted a series of control reactions with **pDTCz-DPmS** as documented in Table 2. The first interrogated the role of the two additives, DIPEA and HE. Both DIPEA and HE are required in addition to **pDTCz-DPmS** to obtain the optimal yield (entries 2 and 3 versus 1); the presence of DIPEA contributes more significantly to the yield than the HE. The absence of both additives results only in trace product (entry 4) and the removal of light causes no product to be formed (entry 11). These findings are consistent with those of Yang *et al.*[21] These same control experiments were conducted in the absence of **pDTCz-DPmS** (entries 5–8). Expectedly, in the absence of DIPEA, HE and PC the reaction does not work (entry 8); however, as noted above, a moderate yield of 47% was obtained in the absence of **pDTCz-DPmS** (entry 5). Removal of either HE or DIPEA resulted in a reduction of the yield of the

Table 2. ^{1}H NMR yields obtained in the C(sp)-C(sp^{3}) cross-coupling reaction under a various reaction conditions.[a]

Entry	**pDTCz-DPmS** (y/n)	HE (y/n)	DIPEA (y/n)	Wavelength [nm]	^{1}H NMR yield [%]
1	Y	Y	Y	390	73±1
2	Y	N	Y	390	64±1
3	Y	Y	N	390	34±1
4	Y	N	N	390	Trace
5	N	Y	Y	390	47±3
6	N	Y	N	390	33±1
7	N	N	Y	390	27±0
8	N	N	N	390	Trace
9	Y	Y	Y	427	53±1
10	N	Y	Y	427	48±1
11[b]	Y	Y	Y	-	0

[a] Reaction conditions conducted as shown in Figure 3 unless otherwise noted. For further details consult the SI. ^{1}H NMR yields obtained from at least two independent runs with the standard deviation given using 1,3,5-trimethoxybenzene as an internal standard. [b] No light.

background reaction to 27% and 33%, respectively (entries 6 and 7).

Informed by the absorption profile of the reagents and additives (Figure 4), the excitation wavelength was changed from 390 nm to 427 nm, since the former is capable of photoexciting both **pDTCz-DPmS** and HE, while the latter allows selective photoexcitation of HE only. Not surprisingly, both in the presence and absence of **pDTCz-DPmS** at 427 nm excitation, comparable yields were obtained of 53% and 48%, respectively (entries 9 and 10), that are akin to that of the background reaction (entry 5).

Photophysical investigations

The absorption spectra of each component of the reaction in THF were measured (Figure 4). No significant absorption could be observed for DIPEA and NHPI at the irradiation wavelength of 390 nm while PhCCBr shows a very weak absorption tail at 390 nm. By contrast, HE displays an intense absorption band that completely overlaps with the main absorption band of **pDTCz-DPmS**. It is worth noting that under the reaction conditions, the percentage of 390 nm light absorbed by HE is estimated to be 15-times higher in comparison to that of **pDTCz-DPmS**, based on their concentrations and molar extinction coefficients (ε) at this wavelength. As previously mentioned, 427 nm light selectively excites the HE.

To interrogate the mechanism of the reaction, we focused our attention on identifying which species was responsible for the quenching of the excited state of **pDTCz-DPmS**. As such, the steady-state and time-resolved emission of **pDTCz-DPmS** in THF were recorded in the presence of each reaction component. It is worth noting that in the case of HE, a lower concentration was used (Table 3), otherwise the HE fluorescence band would dominate the emission spectrum (Figure S7). In THF, **pDTCz-DPmS** displays a prompt emission decay with a lifetime, τ_p, of 4.3 ns and a delayed emission

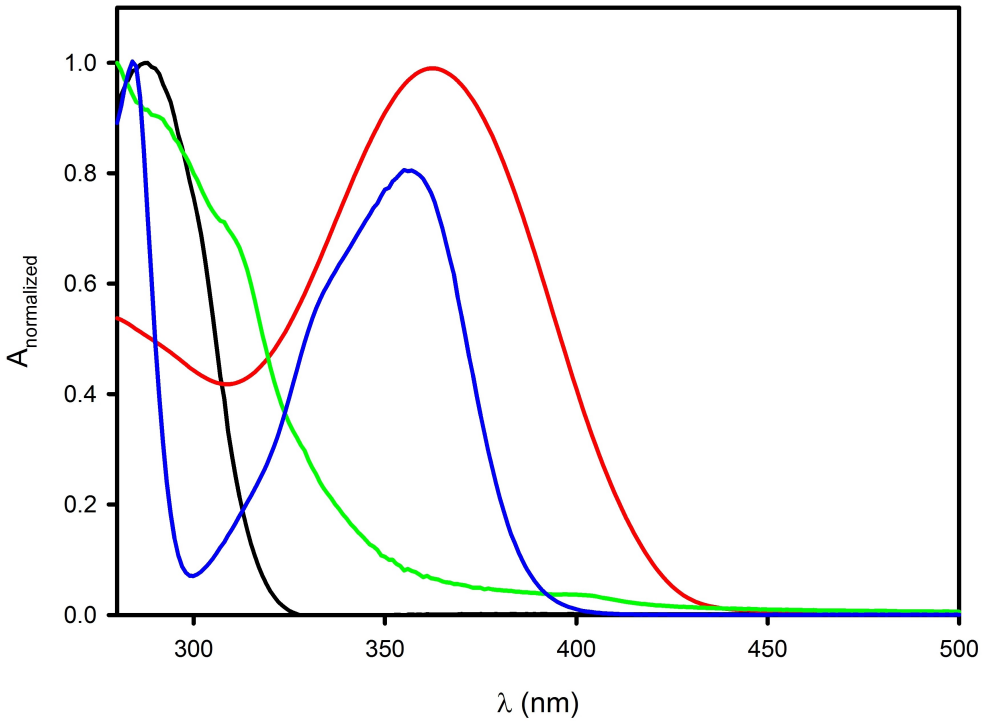

Figure 4. Normalized absorption spectra in THF solution of HE (red), NHPI (black), PhCCBr (green) and **pDTCz-DPmS** (blue).

Table 3. Emission lifetimes for the prompt and delayed fluorescence of **pDTCz-DPmS** in the presence of quenchers.[a]

Quencher	Quencher concentration [mM]	**pDTCz-DPmS** τ_p [ns]	**pDTCz-DPmS** τ_d [μs]
None	0	4.3	3.30
NHPI	4.1	4.0	0.51
DIPEA	3.5	3.5	0.046
PhCCBr	3.7	4.0	0.24
HE	0.052	4.0	1.65

[a] Prompt and delayed lifetimes (τ_p and τ_d, respectively) were recorded at room temperature in deaerated THF using $\lambda_{exc} = 340$ nm.

(TADF) decay with lifetime, τ_d, of 3.30 μs in the absence of oxygen. Significant quenching was observed upon addition of each of the reaction components, although this quenching was focused almost exclusively on the delayed emission of **pDTCz-DPmS** (Table 3). The τ_p remained within 3.5–4.0 ns, reflective of the 4.3 ns lifetime of **pDTCz-DPmS** in the absence of quencher. Instead, τ_d was shown to dramatically decrease from 3.30 μs to between 0.046–1.65 μs, depending on the quencher.

The quenching rate constants, k_q, as estimated from the Stern-Volmer equation, are reported in Table 4.[28] For all quenchers, k_q was very high; on the order of 10^9–10^{10} $M^{-1}s^{-1}$ for the prompt emission quenching and 10^8–10^9 $M^{-1}s^{-1}$ for the delayed emission quenching (Table 4). The weight of the prompt (X^{PROMPT}) and TADF emission (X^{TADF}) quenching was evaluated by comparison of the corresponding k_q for a specific quencher, the lifetimes, and the distribution of the excited state between prompt (Φ^{PROMPT}) and TADF emission (Φ^{TADF}) (see SI for more details). The quenching of the delayed emission is more relevant in all cases (Table 4): X^{TADF} is more than 93% for PhCCBr, NHPI and DIPEA, while is 63% in the case of HE. The TADF emission is mainly quenched by DIPEA (>99.9% under the reaction conditions), implying that in the C(sp)-C(sp^3) cross-coupling reaction, **pDTCz-DPmS** is reductively quenched by DIPEA.

To rationalize the experimental evidence that the reaction proceeds also in the absence of **pDTCz-DPmS**, where HE is the predominant species absorbing the excitation light, we studied the quenching of the HE fluorescence in the presence of the other reactants in THF solution. Since the fluorescence of HE shows a very short lifetime (~0.2 ns), significant changes in its decay are hardly detectable with our experimental setup.

Table 5. Photophysical parameters of the quenching processes for HE in THF solution.

	HE	
Quencher	k_q [$M^{-1}s^{-1}$]	Quenching contribution [%]
NHPI	1.9×10^{10}	35
DIPEA	1.2×10^{8}	0.4

Therefore, for an estimation of the quenching constants, we monitored the decrease of the emission quantum yields in the steady-state photoluminescence spectra. The concentration of HE employed was 2.55×10^{-3} M and the concentrations of the other reagents were the same as in the reaction conditions (0.2–0.4 M). In the case of PhCCBr, we were unable to estimate the quenching constant because its absorption spectrum overlaps with the fluorescence of HE, causing strong reabsorption effects. The quenching rate constants for NHPI and DIPEA are reported in Table 5. The efficiency of quenching of the HE fluorescence was calculated as 35% for NHPI and 0.40% for DIPEA, indicating that NHPI is the predominant quencher of the emission of HE.

To further probe the possible mechanistic pathways of the reaction, the UV-Vis absorption spectrum and ^{1}H NMR spectrum of **pDTCz-DPmS** were each monitored upon addition of increasing equivalents of HE (Figure S5 and S10, respectively). In the former, the absorption spectrum of HE was simply superimposed onto that of **pDTCz-DPmS** while in the ^{1}H NMR spectrum, no discernible changes could be determined. These experiments imply that in the ground state, no species is formed between **pDTCz-DPmS** and HE, ruling out the possibility of an EDA complex. We also evaluated whether an EDA complex forms between NHPI and HE. After mixing the two compounds no significant changes are observed in the UV-Vis absorption spectra (Figure S7) and no new bands related to the EDA complex were observed.

Discussion

Based on these photophysical investigations, a possible catalytic mechanism in operation for the C(sp)-C(sp^3) cross coupling reaction under our reaction conditions is presented in Scheme 2. After photoexcitation, **pDTCz-DPmS** is proposed to be reductively quenched by DIPEA, with closure of the photo-

Table 4. Photophysical parameters of the quenching processes for **pDTCz-DPmS** in degassed THF solution.

	pDTCz-DPmS (prompt fl.)			**pDTCz-DPmS** (TADF)		
	k_q [$M^{-1}s^{-1}$]	Quenching contribution [%]	Relative quenching X^{prompt} [%]	k_q [$M^{-1}s^{-1}$]	Quenching contribution [%]	Relative quenching X^{TADF} [%]
NHPI	4.2×10^{9}	0.6	7	4.0×10^{8}	53.3	93
DIPEA	1.6×10^{10}	4.2	2	6.1×10^{9}	1.7	98
PhCCBr	5.6×10^{9}	1.1	4	1.0×10^{9}	6.8	96
HE	$>5\times10^{10}$	94	37	5.9×10^{9}	38.2	63

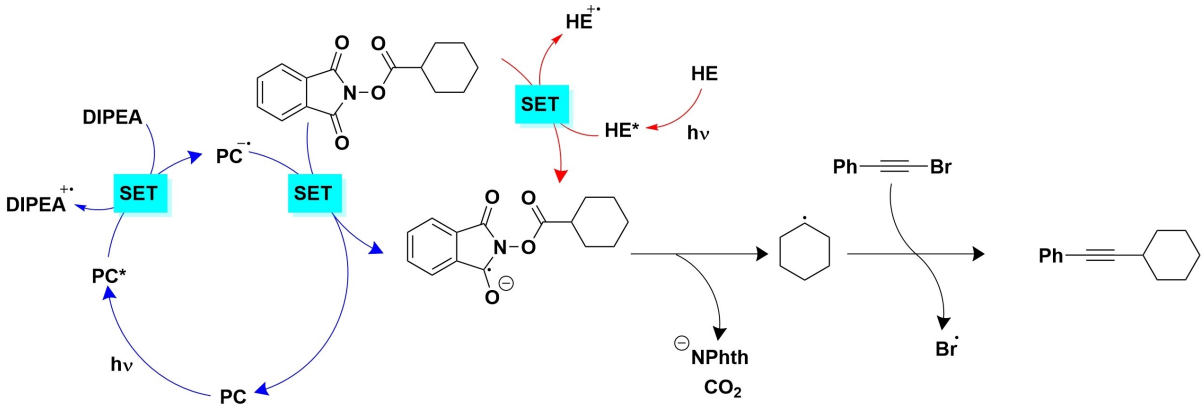

Scheme 2. Proposed reaction mechanism for the C(sp)-C(sp^3) crossing coupling reaction using **pDTCz-DPmS** as the PC under 390 nm irradiation. In blue, the **pDTCz-DPmS** cycle, and in red, the **HE** route.

catalytic cycle occurring by SET from the radical anion of **pDTCz-DPmS** to the NHPI, forming NHPI$^{\bullet-}$. This is consistent with the mechanism proposed in Scheme 1, using [Ru(bpy)$_3$](PF$_6$)$_2$ as the PC. Simultaneously, under the 390 nm irradiation, HE is also photoexcited, and is oxidatively quenched by the NHPI, also producing NHPI$^{\bullet-}$. Subsequent decarboxylative fragmentation releases the alkyl radical, which adds to the alkynyl bromide, generating the target product.

The significant difference between **pDTCz-DPmS** and HE is that the former acts photocatalytically, namely it operates in such a way as to be regenerated during the course of the reaction. By contrast, HE effectively acts as a stoichiometric photoreductant. To further confirm this, we monitored the reaction in the absence of PC by ^{1}H NMR spectroscopy (Figure S11). During the reaction, a quartet at 4.39 ppm is seen to increase in magnitude. This quartet is indicative of the aromatized HE (diethyl 2,6-dimethylpyridine-3,5-dicarboxylate, Figure S12);[29] further, observed singlets at 8.67 and 2.85 ppm are also associated with the oxidised HE generated during the reaction.

The combination of two synergistic mechanisms leading to enhanced product yields is unusual in photoredox catalysis. Although much research has been devoted to dual catalysis, this involves the combination of a PC with an additional catalyst, such as a transition metal catalyst or hydrogen atom transfer catalyst.[2,30] In this form of dual catalysis, both catalysts are typically required in order for the target product to be formed, while in our study we demonstrate that both **pDTCz-DPmS** and HE work independently of one another, contributing synergistically to the product yield.

HEs are a common and versatile additive in the photocatalysis literature.[31] Predominately, HEs are used as an electron donor and/or proton source in photoredox catalysis. If, however, they have an alkyl group in the 4-position, they can also be useful as radical precursors, and through an oxidative fragmentation mechanism, have been employed as alkylating agents, generated through both photocatalysis and direct irradiation.[32] There are also examples of HEs being used as stoichiometric photoreductants[33] but as far as we are aware, there are no reports of HEs being used as photoreductants in combination with an external PC. Therefore, the mechanism proposed in this C(sp)-C(sp^3) reaction is distinct to those reported in the literature in that product forms as a result of photoexcitation of both **pDTCz-DPmS** and HE, independently, with the greatest product yields obtained when both species are present.

The elucidation of the mechanism in operation is further exacerbated by the observation that the reaction proceeds in the absence of both **pDTCz-DPmS** and HE (entry 7; Table 2), although at a low yield of 27%. Based on the UV-Vis absorption spectra (Figure 4) of the remaining reactants, only PhCCBr has an absorption band at the excitation wavelength and given that the reaction does not operate in the absence of light (entry 11, Table 2), we therefore conclude that photoinduced homolytic cleavage of the C–Br bond must occur to initiate the C(sp)-C(sp^3) reaction. Since the reaction also does not proceed in the absence of PC, HE and DIPEA (entry 8; Table 2), the addition of DIPEA must be necessary to act as a proton shuttle to form the target product.

Conclusions

Replicating literature studied photocatalysis reactions is not without issues. The variation in photoreactor set-up means that a yield reported using one photoreactor may not be representative of the yield achieved using an alternative set-up. As such, it is imperative that benchmarking of literature reactions using a consistent photoreactor setup be conducted to permit an accurate comparison of performance. In our case, we observed a background reaction in the absence of PC, despite the report of none existing. This C(sp)-C(sp^3) cross-coupling reaction can be promoted either photocatalytically (**pDTCz-DPmS**) or using a sacrificial photoreductant (HE), substantiated by Stern-Volmer quenching studies. Moreover, the greatest product yield occurs when these mechanistic pathways work in tandem, something that is rarely identified in the photocatalysis literature. This study provides important lessons to the photocatalysis community to always consider testing for background reactions, even when the literature reports none, to carefully assess the

potential of each reagent to quench the excited state of the PC and to corroborate reaction yields with relative quenching kinetics.

Supporting Information

Electronic supplementary information available: synthetic procedures, NMR spectra, UV-Vis absorption spectra, luminescence studies, and photocatalysis set-up.

Acknowledgements

We are grateful to the University of St Andrews, Syngenta and the EPSRC Centre for Doctoral Training in Critical Resource Catalysis (CRITICAT) for financial support [Ph.D. studentship to "M.B."; Grant code: EP/L016419/1]. We thank Umicore AG for the gift of materials. E.Z.-C. and P.C. acknowledge the European Union H2020 research and innovation program under the Marie Skłodowska Curie Grant Agreement (PhotoReAct, No 956324).

Conflict of Interests

The authors declare no conflict of interest.

[1] M. A. Bryden, E. Zysman-Colman, *Chem. Soc. Rev.* **2021**, *50*, 7587–7680.
[2] J. Twilton, C. C. Le, P. Zhang, M. H. Shaw, R. W. Evans, D. W. C. Macmillan, *Nat. Chem. Rev.* **2017**, *1*, 0052.
[3] J. H. Shon, T. S. Teets, *Comments Inorg. Chem.* **2020**, *40*, 53–85.
[4] G. E. M. Crisenza, P. Melchiorre, *Nat. Commun.* **2020**, *11*, 803–806.
[5] N. A. Romero, D. A. Nicewicz, *Chem. Rev.* **2016**, *116*, 10075–10166.
[6] C. K. Prier, D. A. Rankic, D. W. C. MacMillan, *Chem. Rev.* **2013**, *113*, 5322–5363.
[7] K. Villa, J. R. Galán-Mascarós, N. López, E. Palomares, *Sustain. Energy Fuels* **2021**, *5*, 4560–4569.
[8] S. Roslin, L. R. Odell, *Eur. J. Org. Chem.* **2017**, 1993–2007.
[9] T. Noel, E. Zysman-Colman, *Chem. Catal.* **2022**, *2*, 468–476.
[10] D. Ziegenbalg, A. Pannwitz, S. Rau, B. Dietzek-Ivanšić, C. Streb, *Angew. Chem. Int. Ed.* **2022**, *61*, e2021141.
[11] T. D. Svejstrup, A. Chatterjee, D. Schekin, T. Wagner, J. Zach, M. J. Johansson, G. Bergonzini, B. König, *ChemPhotoChem* **2021**, *5*, 808–814.
[12] G. Pirgholi-Givi, S. Farjami-Shayesteh, Y. Azizian-Kalandaragh, *Phys. B* **2020**, *578*, 411886.
[13] Y. Murillo-Acevedo, J. Bernal-Sanchez, L. Giraldo, R. Sierra-Ramirez, J. C. Moreno-Piraján, *ACS Omega* **2019**, *4*, 19605–19613.
[14] F. Draper, E. H. Doeven, J. L. Adcock, P. S. Francis, T. U. Connell, *J. Org. Chem.* **2023**, *88*, 6445–6453.
[15] A. J. Rieth, M. I. Gonzalez, B. Kudisch, M. Nava, D. G. Nocera, *J. Am. Chem. Soc.* **2021**, *143*, 14352–14359.
[16] M. Marchini, A. Gualandi, L. Mengozzi, P. Franchi, M. Lucarini, P. G. Cozzi, V. Balzani, P. Ceroni, *Phys. Chem. Chem. Phys.* **2018**, *20*, 8071–8076.
[17] K. Donabauer, M. Maity, A. L. Berger, G. S. Huff, S. Crespi, B. König, *Chem. Sci.* **2019**, *10*, 5162–5166.
[18] T. U. Connell, C. L. Fraser, M. L. Czyz, Z. M. Smith, D. J. Hayne, E. H. Doeven, J. Agugiaro, D. J. D. Wilson, J. L. Adcock, A. D. Scully, D. E. Gomez, N. W. Barnett, A. Polyzos, P. S. Francis, *J. Am. Chem. Soc.* **2019**, *141*, 17646–17658.
[19] M. A. Bryden, F. Millward, T. Matulaitis, D. Chen, M. Villa, A. Fermi, S. Cetin, P. Ceroni, E. Zysman-Colman, *J. Org. Chem.* **2023**, *88*, 6364–6373.
[20] P. L. Dos Santos, D. Chen, P. Rajamalli, T. Matulaitis, D. B. Cordes, A. M. Z. Slawin, D. Jacquemin, E. Zysman-Colman, I. D. W. Samuel, *ACS Appl. Mater. Interfaces* **2019**, *11*, 45171–45179.
[21] J. Yang, J. Zhang, L. Qi, C. Hu, Y. Chen, *Chem. Commun.* **2015**, *51*, 5275–5278.
[22] J. Luo, X. Zhang, J. Lu, J. Zhang, *ACS Catal.* **2017**, *7*, 5062–5070.
[23] W. Huang, X. Cheng, *Synlett* **2017**, *28*, 148–158.
[24] C. Zheng, Y. Wang, Y. Xu, Z. Chen, G. Chen, S. H. Liang, *Org. Lett.* **2018**, *20*, 4824–4827.
[25] C. Minozzi, A. Caron, J. C. Grenier-Petel, J. Santandrea, S. K. Collins, *Angew. Chem. Int. Ed.* **2018**, *57*, 5477–5481.
[26] E. G. Moschetta, T. Knauber, F. Susanne, F. Lévesque, L. J. Edwards, *Nat. Commun.* **2020**, *11*, 804–807.
[27] Y. Zhang, M. Heberle, M. Wächtler, M. Karnahl, B. Dietzek, *RSC Adv.* **2016**, *6*, 105801–105805.
[28] V. Balzani, P. Ceroni, A. Juris, *Photochemistry and Photophysics: Concepts, Research, Applications*, *1st ed.*, Wiley-VCH, **2014**.
[29] N. Nakamichi, Y. Kawashita, M. Hayashi, *Synthesis* **2004**, *7*, 1015–1020.
[30] K. L. Skubi, T. R. Blum, T. P. Yoon, *Chem. Rev.* **2016**, *116*, 10035–10074.
[31] P. Z. Wang, J. R. Chen, W. J. Xiao, *Org. Biomol. Chem.* **2019**, *17*, 6936–6951.
[32] L. Buzzetti, A. Prieto, S. R. Roy, P. Melchiorre, *Angew. Chem. Int. Ed.* **2017**, *56*, 15039–15043.
[33] D. Chen, L. Xu, T. Long, S. Zhu, J. Yang, L. Chu, *Chem. Sci.* **2018**, *9*, 9012–9017.

Manuscript received: June 29, 2023
Revised manuscript received: August 16, 2023
Accepted manuscript online: August 16, 2023
Version of record online: ■■, ■■

ACES Asian Chemical Editorial Society

ASIAN JOURNAL OF ORGANIC CHEMISTRY
Research Article

RESEARCH ARTICLE

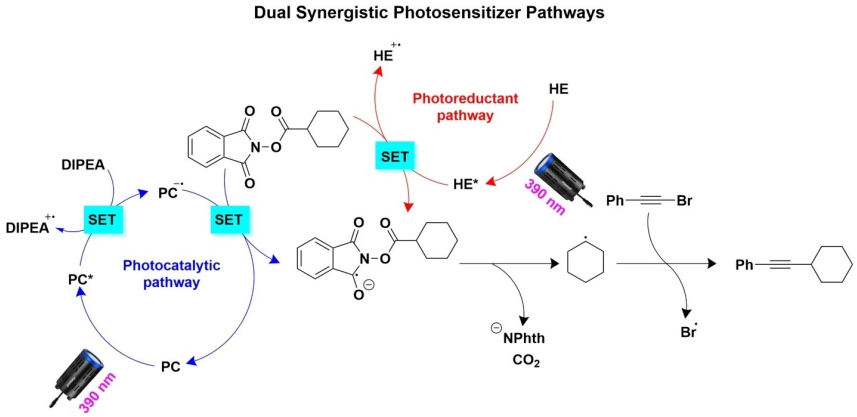

The image shows a proposed mechanism for the formation of the C(sp)-C(sp3) cross-coupled product from bromoalkynes and N-(acyloxy)phthalimde. The mechanism involves both a photocatalytic cycle and a separate photoreductant pathway, employing a Hantzsch ester as a sacrificial photoreductant.

M. A. Bryden, Dr. M. Villa, Dr. A. Fermi, Prof. Dr. P. Ceroni, Prof. Dr. E. Zysman-Colman**

1 – 8

Dual Photosensitizer Cycles Working Synergistically in a C(sp)-C(sp^3) Cross-Coupling Reaction